

Synthesis and Characterization of Submicron PMMA Particles Containing Rare Earth Ions on the Surface

Jun Hu,^{1,2} Hui Zhao,^{1,2} Qijin Zhang,^{1,2} Weidong He²

¹Structure Research Laboratory, University of Science and Technology of China, Hefei 230026, Anhui, China

²Department of Polymer Science and Engineering, University of Science and Technology of China, Hefei 230026, Anhui, China

Received 15 July 2002; accepted 27 September 2002

ABSTRACT: Emulsifier-free emulsion polymerization was adopted to synthesize rare earth containing submicron polymer particles under microwave irradiation. To control the size and distribution of the particle, the relationship between reaction time, monomer content, and particle radius was studied for the polymerization of methyl methacrylate (MMA) in the absence and presence of rare earth ions, in which water was used as solvent, and potassium persulfate was used as initiator. In the latter polymerization, the solution of MMA and europium octanoate (EOA) was used instead of MMA itself as EOA can be dissolved in MMA within certain concentrations, and the result shows that the polymerization process is affected by existence of EOA except when the amount of MMA is 2 ml. For particles con-

taining rare earth ions, characterization shows that mole percentage of Eu(III) ion in the surface layer with a thickness of 5 nm, which is estimated from X-ray photo electron spectroscopy (XPS), is always larger than the value estimated by inductively coupled plasma atomic emission spectrometer (ICP-AES) for the whole particle, indicating that surface enrichment of rare earth ions took place during the polymerization. Further characterization by XPS depth measurement after Ar⁺ sputtering shows the same result. © 2003 Wiley Periodicals, Inc. *J Appl Polym Sci* 89: 1124–1131, 2003

Key words: composites; emulsion polymerization; light scattering; particle size distribution

INTRODUCTION

Rare earth containing polymers have been extensively studied with respect to applications for luminescence, laser materials,^{1–4} color screens, and rare earth containing optical fibers.^{5,6} Usually, the rare earth containing polymer materials are gained through bulk polymerization. However, colloidal particles have long been used as the major components of industrial products such as foods, inks, paints, coatings, papers, cosmetics, photographic films, and rheological fluids.⁷ Recently, emulsifier-free emulsion polymerization attracted much research interest. Having many advantages, such as a narrow size distribution and a clean surface,^{8,9} latex particles obtained by the polymerization have many potential applications in fabrication of optical materials, for example, photonic crystals.^{10–14}

However, emulsifier-free emulsion polymerization proceeds slowly because fewer particles are produced than normal emulsion polymerization.¹⁵ Compared with normal heating, microwave heating is homogeneous and powerful. Some interesting phenomena can be observed when it is used in emulsifier-free emulsion polymerization.^{16–17} The results indicate a reac-

tion under microwave heating is faster than conventional method. However, to our knowledge, this method has not been used to prepare rare earth containing colloidal particles.

Generally speaking, inorganic ions, such as rare earth ions, are not compatible with organic polymers. To change the situation mentioned above, two methods have often been adopted: First, the chelate or the organic salt of rare earths was made and then mixed with the polymers¹⁸; second, the rare earth ion containing monomers were synthesized and then polymerized.^{4,9} To get homogeneous distribution, another method was developed, in which organic salts of rare earth ions were first mixed with monomer and then by bulk polymerization of methyl methacrylate (MMA) containing the ions, poly(methyl methacrylate) (PMMA), doped with rare earth ions. For example, neodymium octanoate used to be adopted in such a polymerization, and PMMA with homogeneously doped ions was obtained at a concentration of Nd³⁺ of 70 ppm.²⁰ In this work, within the concentration range in which solution of europium octanoate (EOA) in MMA can be obtained, submicron particles of PMMA doped with Eu³⁺ was synthesized by emulsifier-free emulsion polymerization under microwave irradiation. Characterization of such particles was made by X-ray photoelectron spectroscopy (XPS) and inductively coupled plasma atomic emission spectrometer

Correspondence to: Q. Zhang (zqjm@ustc.edu.cn).

(ICP-AES), and halo configuration model for such particles is put forward based on discussion of the result.

EXPERIMENTAL

Materials

MMA [analytical reagent (AR)] was washed with a 10% sodium hydroxide (NaOH) aqueous solution and distilled water three times, dried with anhydrous sodium sulfate, and then distilled in vacuum. It was stored in a refrigerator before use. Potassium persulfate (KPS) was recrystallized from its saturated aqueous solution at 40°C. (MMA, NaOH, and KPS were obtained from the Shanghai Chemical Reagent Co., Ltd. Shanghai, China). EOA [$\text{Eu}(\text{C}_7\text{H}_{15}\text{COO})_3$] was synthesized from Eu_2O_3 , according to the procedure reported before.²¹

Microwave emulsifier-free emulsion polymerization

A 250-ml three-necked flask equipped with a mechanical stirrer, a nitrogen inlet, and a special condenser was placed in a modified microwave oven and then distilled water (100 ml) was added. The water was heated to a high temperature ($\sim 70^\circ\text{C}$) by 450 W for 3 min. With nitrogen used as protective gas, 10 ml KPS solution (0.02 wt %) and 2–10 ml MMA were added, respectively. The temperature of the reaction mixture was kept at $\sim 80^\circ\text{C}$ by 80 W. A stable emulsion was obtained after the reaction stood for 1–5 h.

The emulsion was centrifuged with an ultracentrifuge (Beckman-Coulter Ltd., J21M) at 12,000 rpm for 20 min. Product of centrifuge was washed with methanol (AR) and centrifuged again to remove the impurity and unreacted monomer. Then, the product was dried in a vacuum at 50°C .

Within a certain concentration range, EOA can be dissolved into MMA at 80°C . Polymerizing with this solution, rare earth containing PMMA particles can be obtained by the microwave emulsifier-free emulsion polymerization in the same way as described above.

Normal emulsifier emulsion polymerization

Distilled water (100 ml) was added to a flask equipped with an electromagnetic stirrer, a nitrogen inlet, and a condenser, and was heated to 80°C in an oil bath while being purged with nitrogen. Ten milliliters of KPS (0.02 wt %) and 8 ml MMA were added, respectively. The temperature of the reaction mixture was kept at $80 \pm 2^\circ\text{C}$. A stable white emulsion was obtained after the reaction stood for 6 h under a nitrogen atmosphere.

Determination of particles size and size distribution

The emulsion was thinned with deionized water to a desirable concentration. After the sample stood at

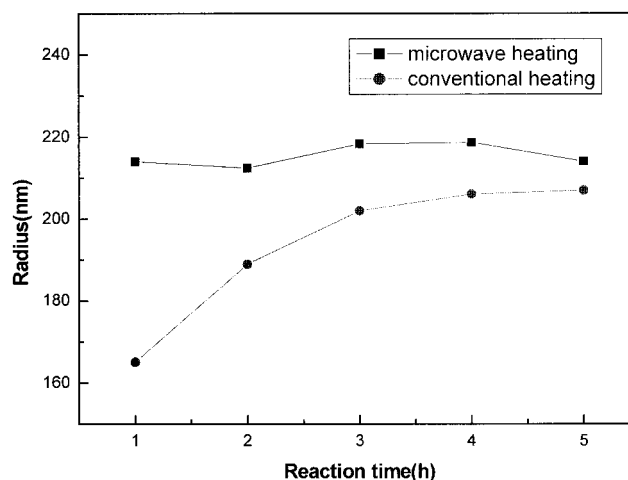


Figure 1 Comparison of changing tendency of particle size with reaction time. —■— and —●— represent the reaction under microwave heating and conventional heating, respectively. Both reactions were kept at $\approx 80^\circ\text{C}$ with the same monomer amount (8 ml) and the same amount of initiator (10 ml 0.02 wt % KPS).

25°C in the cell chamber for 10 min, the radius and the size distribution were determined by a modified commercial LLS spectrometer (ALV/SP-125) equipped with an ALV-5000 multi- τ digital time correlator and a solid-state laser (ADLAS DRY 425 II, out power = ≈ 400 mV at $\lambda = 532$ nm).

Characterization of submicron particles

Eu content on particle surface was measured by an X-ray photoelectron spectroscopy electron spectrometer (XPS, VG Scientific Ltd., ESCalab MKII). At target was used in the experiment. Depth profile was measured with an Ar^+ sputtering sample. About 10 nm of surface was removed after 3 min of sputtering. Eu content in whole particles was measured by ICP-AES (Thermo Jarrell Ash Corp., Atomscan Advantage). A spectrofluorophotometer (SHIMADZU, RF-5301PC) was used to measure luminescence of rare earth containing submicron particles. Samples were excited by light at 396 nm.

RESULTS AND DISCUSSION

Comparison with conventional emulsifier-free emulsion polymerization

A certain amount of monomer and initiator was added into the reaction vessel. Three minutes later, the reaction mixture under microwave heating gradually turned white, whereas the same mixture under conventional heating did so 7 min later. Some mixture was drawn to measure particle size after every hour's interval. Results are shown in Figure 1. It is clearly seen from Figure 1 that the reaction

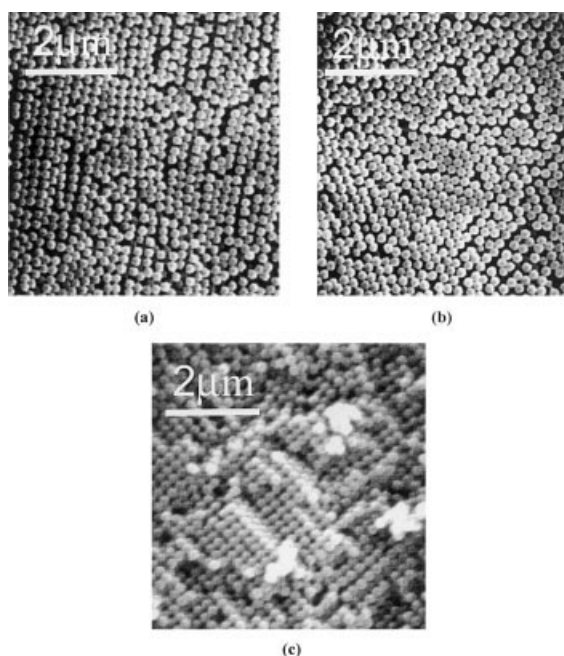


Figure 2 SEM images of particles acquired from different reactions. (a) Particles under conventional heating; (b) particles under microwave heating; (c) particles with rare earth ion.

under microwave heating is faster than that under conventional heating. However, after both of the two reactions had finished, the final particle sizes obtained from them are nearly same. This indicates that the mechanism of two reactions is the same except for the reaction rate. Under microwave irradiation, polar molecules would move along with the frequency of the irradiation, other than random movement under the heating. This is a possible reason for a quicker reaction rate under microwave heating, although the macroscopic temperature of two reaction systems was controlled identically by adjusting irradiation time of the microwave polymerization. SEM images [Fig. 2 (a, b)] of particles acquired from these two reactions are similar to each other, too. Other workers also mentioned that microwave irradiation could not cause any shift in equilibrium of chemical reactions.²²

The content and distribution of rare earth ions in particles made by microwave emulsifier-free emulsion polymerization

Solution of EOA in MMA was used in synthesis of rare earth containing PMMA particles by microwave emulsifier-free emulsion polymerization instead of MMA itself. During the polymerization, it has been found that the ion content in particles is usually different from the ion content amount of the ion dissolved in monomer before the polymerization. The main reason may be that part of EOA did not enter the polymer, but adhered to the flask. To accurately determine the content and distribution of the ion, measurements should be performed on samples of rare earth containing submicron particles. Mole percentage of Eu(III) ion on the surface of the particle (C_{MPE}) and concentration of Eu(III) ion in the whole particle (W_{ECW}) can be measured by XPS and ICP-AES, respectively. The data obtained by these two methods are listed in Table I for samples 1–4.

In XPS experiments, it has been known that only the atom in escape depth can be detected. As for electron of Eu3d5/2, escape depth can be calculated with the method established by Seah and Dench²³ as about 5 nm. The data from XPS measurement (C_{MPE}) listed in Table I are concerned with such a surface with its thickness of 5 nm.

The mole percentage of Eu(III) ion on the surface of the particle (C_{MPE}) can also be calculated by ICP-AES measurement, from which the total Eu(III) ion weight concentration (W_{ECW}) can be obtained, considering the thickness of the surface as escape depth. During the deduction in terms of results from ICP-AES measurement, two hypotheses are used. One is that density change brought by rare earth ion existence is ignored because the content of rare earth ion is small. Even on the particle surface, as can be seen in calculation below, the weight concentration is less than 5%. To simplify calculation, the same density is applied in each part of the particle. Therefore, it is easy to translate each other between weight concentration and volume concentration. The other is that distribution of Eu(III) ion on particle surface is homogenous. Therefore, mole percentage given by XPS can be considered

TABLE I
 C_{MPE} , W_{ECW} , S_{ECS} , and Radius of Eu-Containing Particles^a

	C (mol %)	W (g/g)	Radius (nm)	S (g/g)
Sample 1 (30000ppm)	0.23	0.000768	133	0.0071
Sample 2 (10000ppm)	0.3	0.002769	84	0.0164
Sample 3 (45000ppm)	0.47	0.003617	96	0.0245
Sample 4 (45000ppm)	0.51	0.004046	151	0.042

^a All reactions were kept at $\approx 80^\circ\text{C}$ with the same monomer amount (2 ml) and the same amount of initiator (10 ml 0.02 wt % KPS). Certain amount Europium Octanoate [$\text{Eu}(\text{C}_7\text{H}_{15}\text{COO})_3$] was dissolved in MMA at 80°C .

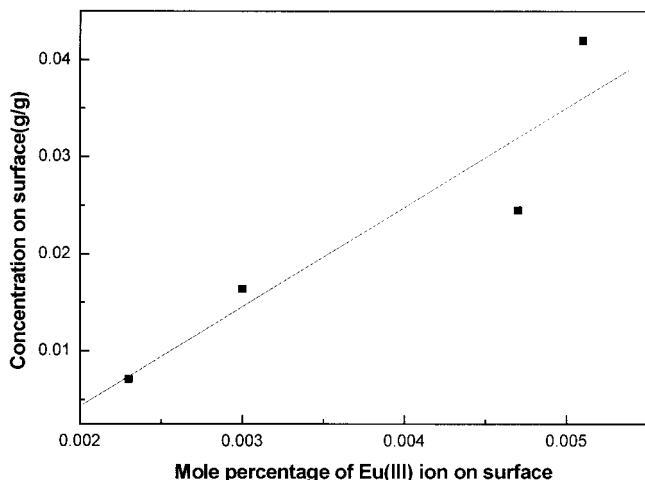


Figure 3 Schematic description of rare earth doped polymer particles. Red points represent rare earth ion and an outer layer with blue color represents escape depth of Eu 3d5/2, in which Eu(III) ion can be detected by XPS.

as a percentage of the whole surface, although area, which is scanned, is a part of the particle surface.

If distribution is homogenous, for example, C_{MPE} of sample 3 is 0.034 (mol %) according to this calculation. Obviously, the value is too small compared with the experimental value of sample 3 detected by XPS. It is reasonable to consider that Eu(III) ion distributed mainly on surface. To describe quantitatively the distribution of Eu(III) ion on the surface of submicron particles, a concept of Eu(III) ion concentration on surface [S_{ECS} (g/g)] is proposed, which means the weight concentration of Eu(III) ion is on the particle surface with a thickness of 5 nm. It can be calculated from the weight concentration in whole particles (W_{ECW}), obtained by ICP-AES under the same assumptions described above. When particle radius is R , the volume of the layer is $1 - [(R - 5nm)^3/R^3]$ as the whole volume of particle is supposed as 1. It can be lead to

$$S_{ECS} = \frac{W_{ECW}}{1 - [(R - 5nm)^3/R^3]} \quad (1)$$

S_{ECS} values for all samples calculated from this equation are listed in Table I. Figure 3 shows the relationship between S_{ECS} values and C_{MPE} values obtained from XPS measurement. A linear relationship can be seen and slope is 10.23 by linear fit.

From the principle of XPS, it has been known that values between S_{ECS} and C_{MPE} should be in the relation described by:

$$S_{ECS} = \frac{M_{Eu}}{M_{MMA}} NC_{MPE} \quad (2)$$

where M_{Eu} is atomic weight of Eu; M_{MMA} is molecular weight of MMA; and N is the number of C and O atoms of a MMA molecule (because H atom cannot be detected by XPS).

As it is known that $M_{Eu} = 152$, $M_{MMA} = 100$, and $N = 7$, respectively, from eq (2), one linear relationship, $S_{ECS} = 10.64C_{MPE}$, can be obtained. The experimental value is very close to the theoretical value. It indicates that the Eu(III) ion distributes mainly on the particle surface, as shown in the schematic model given by Figure 4.

The reason for this phenomenon is probably that the alkyl chain in $Eu(C_7H_{15}COO)_3$ is hydrophobic, so it is apt to enter the interior of particles. Although Eu^{3+} is hydrophilic, it stayed on the surface of particles. The straight line plotted in Figure 3 does not pass the origin. It may be caused by data error from XPS and the hypothesis of homogenous density. There is little rare earth ions within particles, as shown in Figure 4.

Influence of Ar^+ sputtering to particles' XPS measurement also proves the model given by Figure 4. Before and after Ar^+ sputtering of the sample, XPSs were measured for the same sample. From Figure 5, it is obvious that the peak area of XPS after sputtering is smaller than the peak area before sputtering, which indicates that the content of Eu(III) ion decreases on the particle surface after Ar^+ sputtering because part of the surface and some Eu ions were removed. However, it is impossible to remove all Eu ions on the surface because the particle surface is spherical and the measurement angle is larger than the sputtering angle. XPS data is 0.33% after Ar^+ sputtering, whereas before sputtering the data are 0.48%.

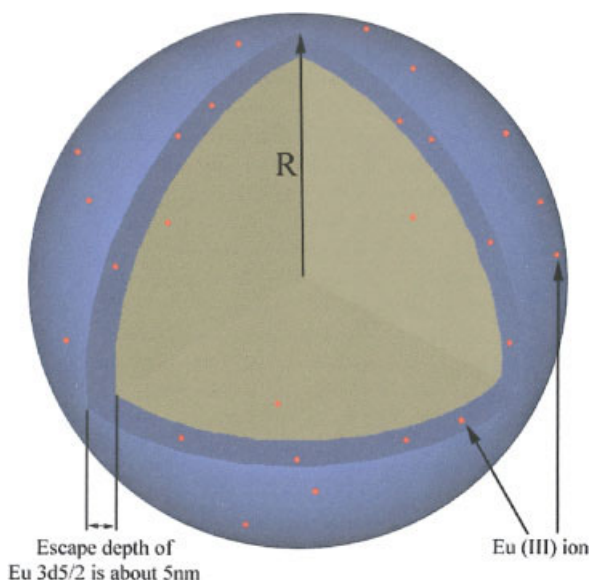


Figure 4 S_{ECS} - C_{MPE} relationship. S_{ECS} is Eu concentration on surface calculated from ICP-AES's data and C_{MPE} is Eu mole percentage on surface, which were acquired from XPS.

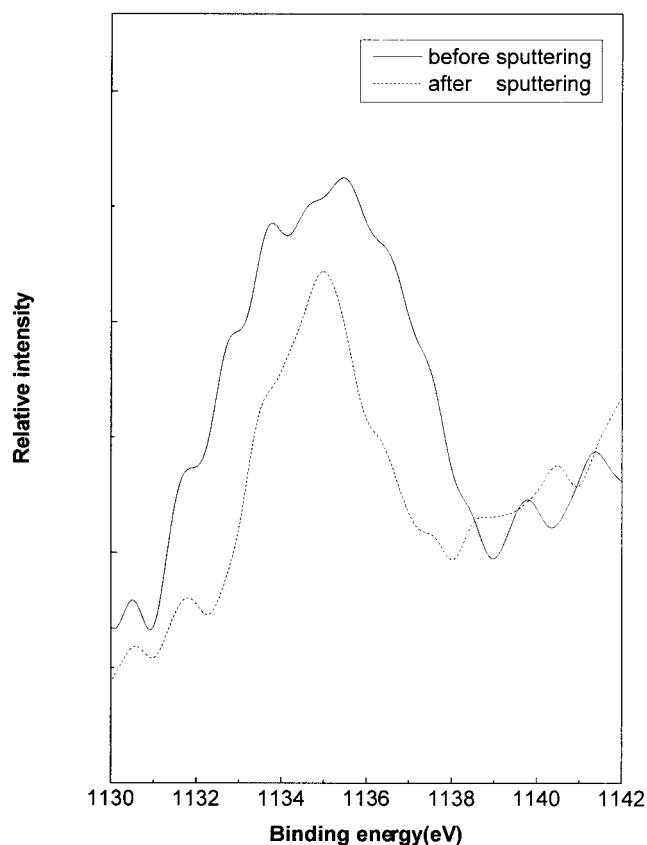


Figure 5 Influence of Ar^+ sputtering to particles' XPS measurement. Solid line is XPS data before sputtering and dash line is XPS data after 3 min Ar^+ sputtering.

Luminescence property of rare earth containing particles

The luminescence properties of rare earth containing particles were measured with a spectrofluorophotometer. EuCl_3 solution was used as reference. Samples were excited at 396 nm, the maximum absorption of Eu(III) ion. The emission spectrum of Eu(III) ion containing particle exhibits the characteristic emissions of Eu(III) ions. As shown in Figure 6, two visible emission peaks centered at 592 and 616 nm, assigned to the $^5\text{D}_0 \rightarrow ^7\text{F}_1$, $^5\text{D}_0 \rightarrow ^7\text{F}_2$ transitions, respectively, were observed. Between these two peaks, the emission at 616 nm from the $^5\text{D}_0 \rightarrow ^7\text{F}_2$ electro-dipole transition is stronger, suggesting low symmetry around the Eu(III) ion in the particles. Because the forbidden $^5\text{D}_0 \rightarrow ^7\text{F}_2$ electro-dipole transition is sensitive to the coordinative environment of Eu(III) ions,^{24,25} the asymmetric microenvironment causes the polarization of the Eu(III) ion under the influence of the electric field of the surrounding ligands, which increases the probability for the electro-dipole transition.²⁵

The size and the size distribution of particles

To find the right condition of obtaining the appropriate size of particles, a different amount of pure MMA

was used in the polymerization first. Results of particle size and its distribution are shown in Figures 7 and 8, respectively. The special-sized particles can be obtained by ceasing the reaction at the right time. From Figure 7 it can be seen that for each monomer amount the particle radius increases with reaction time prolonged. For the system with less monomer, such as 2 or 4 ml, the size of particles quickly reaches the final values within 20 min. From the inset of Figure 6, the same situation can be found for the system with more monomer within 1 h. The fact that the particle size fixes at a certain value indicates that reaction has finished at the starting point of the plateau. This phenomenon is also found in emulsion polymerization, no matter how much monomer has been used. On the other hand, from Figure 7 it can be found that with the amount of monomer increasing, the time required for reaching the final particle size increases. The reason for this phenomenon is that in emulsion polymerization, there is an acceleration of reaction rate at the second half of the reaction,²⁶ which appears at the time dependent on the amount of monomer when other polymerization conditions are identical; the more the monomer, the later the acceleration takes place.

In Figure 7 it can also be found that, when the amount of monomer increased to 10 ml, the size of particles still increases after 5 h. For the emulsifier-free polymerization, the emulsifier was the short polymer chain with part of initiator as end group. In this system, KPS is used as initiator, and the end group is sulfate group, which is of one negative charge. The density of this surface charge depends not only on the amount of initiator, but also on the amount of monomer. The difference in monomer quantity between the system with 10 ml monomer and other systems with

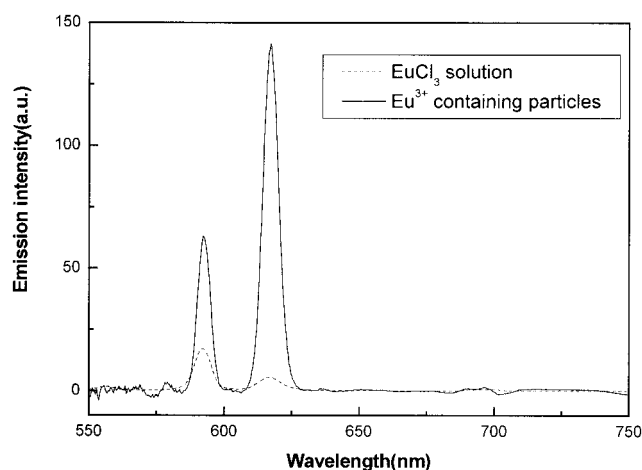


Figure 6 Luminescence spectrum of Eu(III) ion containing particles. Sample was excited at 396 nm. Solid line is emission spectrum of Eu(III) ion containing particles and dash line is emission spectrum of EuCl_3 solution in water.

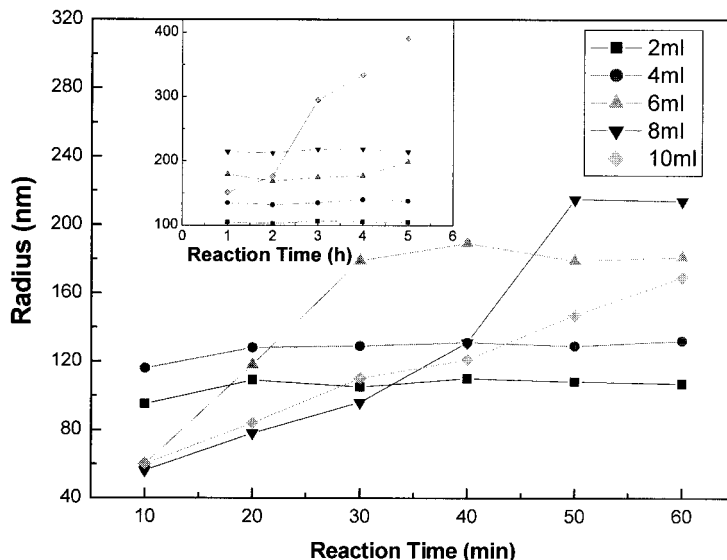


Figure 7 Relationship between particle size and reaction time. All reactions were kept at $\approx 80^\circ\text{C}$ with the same amount of initiator (10 ml 0.02 wt % KPS). Monomer amount is 2, 4, 6, 8, and 10 ml, respectively.

less monomer may be the reason for this point of view. To further investigate this phenomenon, the size distribution of particles was measured at different reaction times for systems with 10 and 2 ml monomers, respectively. The result in Figure 8 shows that the sample obtained from the system with 2 ml monomer has the fixed size distribution within the reaction period, but for the sample with 10 ml monomer the size distribution decreased first, reached lowest value at 3 h, and then increased within the reaction period. For the system with 10 ml monomer, when the same amount of monomer reacted at different particles within 3 h, bigger particles grew slowly and smaller particles grew faster. Under this circumstance, the size

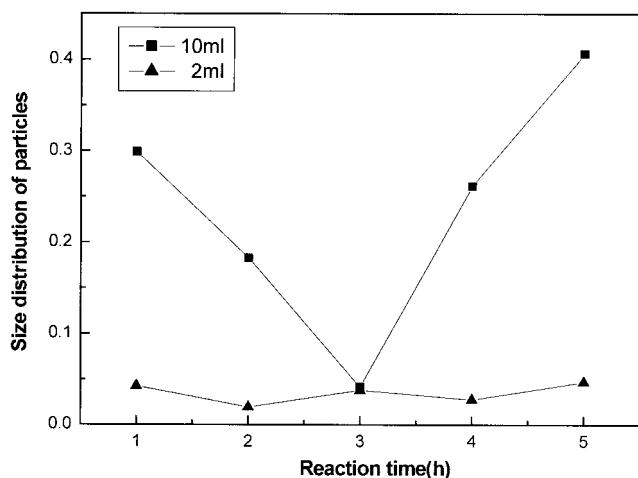


Figure 8 Relationship of distribution and reaction time. All reactions were kept at $\approx 80^\circ\text{C}$ with the same amount of initiator (10 ml 0.02 wt % KPS). Monomer amount is 2 and 10 ml, respectively.

distribution was decreased. At the same time, the surface of particles increases, and the stability of grown particles would decrease because of instability brought about by emulsifier-free and decreasing of the charge density on the surface of grown particles with the polymerization continuing. When the density of electric charge on the surface dropped to a critical value, conglomeration between some particles occurred, and so the distribution rose. Approximate estimation about the critical charge density for the conglomeration can be made for this microwave emulsifier-free emulsion polymerization as shown below.

In an emulsifier-free system, colloidal particles are mainly stabilized with initiator residues. For a small amount of initiator, all initiator residues have their effect on system stabilization. Effect of equilibrium ion can be ignored. Each initiator molecule offers two residues with one negative charge. All residues are hypothesized as distributing on particle surface because they are hydrophilic. From mole amount of initiator, particle surface area, and number of particles, values of electric charge density can be estimated by

$$e_c = 2 \frac{n_{\text{KPS}} N_A e}{A_s N} \text{ (Coulomb/m}^2\text{)} \quad (3)$$

where e_c (C/m²) is the charge density, n_{KPS} (mol) is the mole amount of KPS, N_A is the Avogadro constant, e is the charge of electron ($1.6 \times 10^{-19}\text{C}$), A_s (m²) is the surface area of particle, and N is the number of particles.

The charge densities of samples with different monomer amounts were calculated by eq. (3) and the

TABLE II
Charge Density of Sample with Different Monomer Amount^a

Monomer amount (ml)	n_{KPS} (mol)	Particle radius (nm)	A_s (m ²)	N	Charge density (C/m ²)
2	7.4×10^{-6}	1.0×10^{-7}	1.3×10^{-13}	4.8×10^{14}	0.0228
4	7.4×10^{-6}	1.3×10^{-7}	2.1×10^{-13}	4.3×10^{14}	0.0157
6	7.4×10^{-6}	1.8×10^{-7}	4.1×10^{-13}	2.5×10^{14}	0.0139
8	7.4×10^{-6}	2.2×10^{-7}	6.1×10^{-13}	1.8×10^{14}	0.0130
10	7.4×10^{-6}	2.9×10^{-7}	1.1×10^{-12}	0.98×10^{14}	0.0132

^a N is obtained by volume of single particle dividing monomer amount.

results are listed in Table II. From the results in Figures 7 and 8, it can be concluded that the conglomeration took place at the third hour for the polymerization system with 10 ml monomer. The critical value, e_c , can be obtained with the data of the system with 10 ml monomer and is 0.0132 C/m². In comparison with this value, other e_c values of samples with 2, 4, and 6 ml monomer listed in Table II are all slightly larger. The surface-charge density calculated from data for 8 ml monomer is 0.0130 C/m², lower than the critical e_c , but there is no conglomeration in the system with 8 ml monomer to have been found. This indicates that the estimation is just a primary qualitative work, and there is still much to be accurately done in this aspect.

The size and the size distribution of rare earth containing particles

With the existence of EOA, there are some differences from polymerization in the absence of rare earth ions. Results are shown in Figures 9 and 10. When less monomer was used, for example, 2 ml, the final size of particles, is reached within a short period. This shows

that the polymerization is ended and identical with the polymerization without rare earth compounds. From Figure 2(c), SEM images of rare earth ion containing particles, little difference can be seen between two kinds of particles.

However, when monomer amount increases to 4, 6, and 8 ml, within the time domain adopted in the polymerization the sizes of particles increase with reaction time, as shown in Figure 7 in the absence of rare earth ions. To further investigate this, the size distributions of particles were measured, and the results are shown in Figure 10, from which a similar situation with the 10 ml monomer system in Figure 8 can be found. While the particle radius increases continuously, as for samples with 6 and 8 ml monomer amounts, the size distributions of particles decrease first and increase after a turning point, indicating that particle conglomeration occurs in these reactions too. The white solid can also be seen in the wall of reaction vessel at about 30 and 60 min, respectively, after the reaction starts. The turning point, which means the beginning of the conglomeration, is close to the start

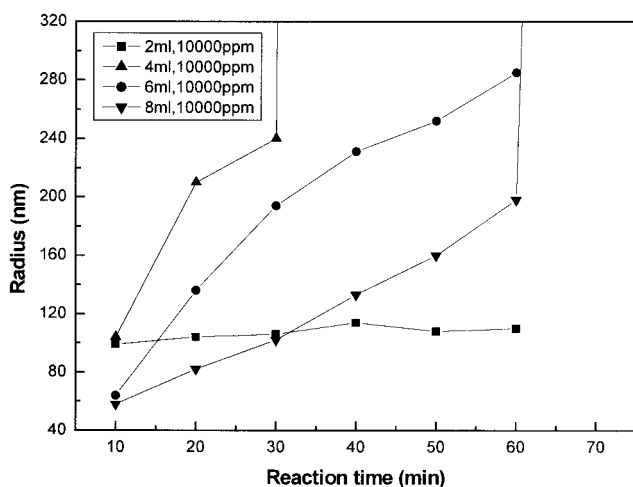


Figure 9 Particle size of reaction with rare earth ion. All reactions were kept at $\approx 80^\circ\text{C}$ with the same amount of initiator (10 ml 0.02 wt % KPS). 10,000 ppm europium octanoate $[\text{Eu}(\text{C}_7\text{H}_{15}\text{COO})_3]$ was dissolved in MMA at 80°C . The solution is used as monomer. Monomer amount is 2, 4, 6, and 8 ml, respectively.

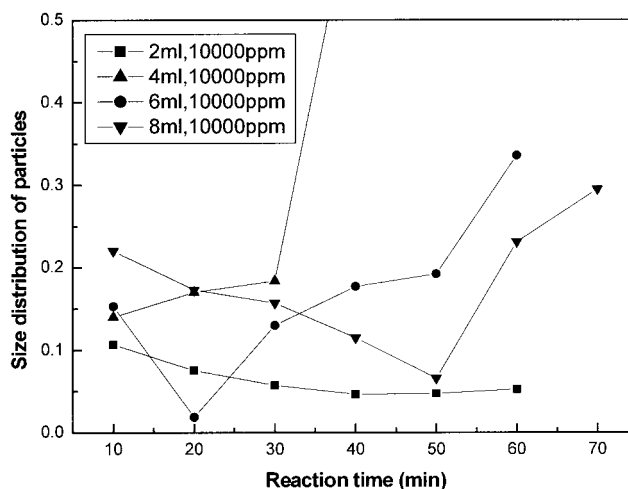


Figure 10 Size distribution of reaction with rare earth ion. All reactions were kept at $\approx 80^\circ\text{C}$ with the same amount of initiator (10 ml 0.02 wt % KPS). 10,000 ppm europium octanoate $[\text{Eu}(\text{C}_7\text{H}_{15}\text{COO})_3]$ was dissolved in MMA at 80°C . The solution is used as monomer. Monomer amount is 2, 4, 6, and 8 ml, respectively.

point of level line in polymerization without rare earth ion. The reason for this difference is the Eu(III) ion has some positive charge, and Eu(III) ion distributes mainly on the surface region of particle, which has been proven above. The negative charge of sulfate is partly neutralized by the positive charge of Eu(III) ion. Reactions follow the mechanism without rare earth ion first. Particles grow and reach the final value. However, because of neutralization caused by Eu(III) ion, the charge density on surface drops to the critical value, resulting in particle conglomeration. As for a sample with 4 ml monomer amount, particle conglomeration occurs between 10 and 20 min, so there is not a turning point to be observed. To the sample with 2 ml monomer, there is little influence on the process of the emulsifier-free emulsion polymerization because the surface charge density of particles without rare earth ion is much higher than the critical value.

CONCLUSION

A new type of rare earth-containing submicron particle was synthesized by microwave irradiation emulsifier-free emulsion polymerization of MMA in the presence of EOA. Experiments indicated that the reaction rate under microwave heating is faster than the reaction rate under conventional heating. Experimental results of XPS and ICP-AES were used to calculate S_{ECS} and C_{MPE} , and a linear relationship between values of S_{ECS} and C_{MPE} was found to have a slope of 10.23, very close to the theoretical value of 10.64. In XPS depth profile, the peak area of Eu after Ar^+ sputtering is smaller than the area before sputtering. Those results show that surface enrichment of rare earth ions took place during the polymerization. Particle conglomeration will occur when an amount of MMA-saturated EOA is more than 4 ml. An amount of 2 ml MMA is appropriate to synthesize rare earth-containing submicron particles.

The National Natural Science Foundation of China (No. 50025309) and the National Committee of Science and Tech-

nology of China (No. RE-05-02) supported this work. The authors gratefully acknowledge the financial support and express thanks to the reviewers for critically reviewing the manuscript and making important suggestions. D. Haiping He, Haidong Zhou, Dongxia Ma, Yue Zhao, and Jie Xu are gratefully thanked for beneficial discussions.

References

1. Piguet, C.; Bunzli, J. C. G.; Bernardinelli, G.; Hopfgartner, G.; Williams, A. F. *J Am Chem Soc* 1993, 115, 8197.
2. Buono-Core, G. E.; Li, H.; Marciniak, B. *Coord Chem Rev* 1990, 99, 55.
3. Qian, D. J.; Yang, K. Z.; Nakahara, H.; Fukuda, K. *Langmuir* 1997, 13, 5925.
4. Galaup, C.; Picard, C.; Cathala, B.; Cazaux, L.; Tisnes, P.; Autiero, H.; Aspe, D. *Helv Chim Acta* 1999, 82, 543.
5. Zhang, Q. J.; Wang, P.; Zhai, Y. *J Appl Polym Sci* 1998, 67, 1431.
6. Zhang, Q. J.; Ming, H.; Zhai, Y. *J Appl Polym Sci* 1996, 62, 887.
7. Hunter, R. J. *Introduction to Modern Colloid Science*; Oxford Univ. Press: Oxford, 1993.
8. Chainey, M.; Hearn, J.; Wilkinson, M. C. *J Polym Sci, Polym Chem Ed* 1987, 25, 505.
9. Peeney, P. J.; Napper, D. H.; Gilbert, R. G. *Macromolecules* 1987, 20, 2922.
10. Park, S. H.; Gates, B.; Xia, Y. N. *Adv Mater* 1999, 11, 462.
11. Rogach, A.; Susha, A.; Caruso, F.; Sukhorukov, G. *Adv Mater* 2000, 12, 333.
12. Gates, B.; Xia, Y. N. *Adv Mater* 2000, 12, 1329.
13. Tarhan, I. I.; Waterson, G. H. *Phys Rev Lett* 1996, 76, 315.
14. Vickreva, O.; Kalinina, O.; Kumacheva, E. *Adv Mater* 2000, 12, 110.
15. Cheng, S.; Li, J.; Ji, Q.; Tongbao, G. *Gaofenzitongbao* 1991, 3, 129.
16. Zhang, W.; Gao, J.; Wu, C. *Macromolecules* 1997, 30, 6388.
17. He, W. D.; Pan, C. Y.; Lu, T. *J Appl Polym Sci* 2001, 80, 2455.
18. N. E. Wolff and R. J. Preeley, *Appl Phys Lett* 1963, 2, 152.
19. Okamoto, Y.; Ueda, Y.; Dzhanibekov, N. F.; Banks, E. *Macromolecules* 1981, 14, 17.
20. Zhang, Q.; Ming, H.; Zhai, Y.; *J Appl Polym Sci* 1996, 62, 887.
21. Xu, W. Y.; Zheng, D. G.; Wang, Y. S.; Zhao, G. W. *Cailiaokexuejinzhan* 1989, 3, 269.
22. Tu, W. X.; Liu, H. F. *J Mater Chem* 2000, 10, 2207.
23. Seah, M. D.; Dench, W. A. *Surf Interf Anal* 1979, 1, 2.
24. Georges, J. *Analyst* 1993, 118, 1481.
25. Kirby, A. F.; Richardson, F. S. *J Phys Chem* 1983, 87, 2544.
26. Trommsdorff, E.; Kohle, H.; Iegally, P. *Macromol Chem* 1947, 1, 169.